Title

ACTIVATION ENERGIES FOR THE DISSOCIATION OF DIATOMIC MOLECULES ARE LESS THAN THE BOND DISSOCIATION ENERGIES

Authors

Johnston, Harold
Birks, John.

Publication Date

1972-06-01

Submitted to Accounts of
Chemical Research

UCRL-20514 Rev.
Preprint

ACTIVATION ENERGIES FOR THE DISSOCIATION OF DIATOMIC MOLECULES ARE LESS THAN THE BOND DISSOCIATION ENERGIES

Harold Johnston and John Birks

June 1972

AEC Contract No. W-7405-eng-48

UCRL-20514 Rev.

DISCLAIMER

ACTIVATION ENERGIES FOR THE DISSOCIATION OF DIATOMIC MOLECULES ARE LESS THAN THE BOND DISSOCIATION ENERGIES[1]

Harold Johnston and John Birks

Department of Chemistry and Inorganic Materials Research Division, Lawrence Berkeley Laboratory, University of California, Berkeley, California

ABSTRACT

Rate constants and activation energies for the thermal dissociation of H_2, N_2, O_2, F_2, Cl_2, Br_2, and I_2 are reviewed and summarized. The observed activation energies in all cases are substantially below the bond dissociation energies. Models are set up in terms of energy-transfer processes between the vibrational states of the reactant, and pertinent constants are evaluated from observed spectroscopic parameters, transport properties, and vibrational relaxation times. Non-equilibrium distributions over vibrational states are calculated. The "ladder climbing" model with dissociation occurring only from the top vibrational state gives an incorrect trend of acitvation energies with temperature. Regardless of the details, each model that permits dissociation from all vibrational states correctly predicts a large decrease in activation energy as temperature increases. At high temperatures, the reaction seriously depletes upper vibrational states, and this decrease in number of states that react causes the rate constant to increase with temperature less rapidly than expected. Thus the activation energy, which is merely a measure of how the rate constant changes with temperature, is lower than the bond dissociation energy.

The dissociation of a homonuclear diatomic molecule X_2 in a "heat bath" of an inert monatomic gas M appears to be a simple chemical process

$$X_2 + M \rightarrow X + X + M \tag{1}$$

In recent years extensive experimental data for H_2, N_2, O_2, F_2, Cl_2, Br_2, and I_2 in Ar and other noble gases have been obtained, Table I, mostly by use of shock tubes. Rate constants $\underline{k}$

$$\underline{k} = -\frac{1}{[M]} \frac{d \ln[X_2]}{dt} \tag{2}$$

have been observed over a wide range of temperature, and Arrhenius activation energies have been evaluated

$$\underline{E} = -\underline{R} \frac{d \ln \underline{k}}{d(1/\underline{T})} \quad , \quad \underline{k} \approx \underline{A} \exp(-\underline{E}/\underline{RT}) \tag{3}$$

An interesting feature of the data is that in each case the activation energy is substantially less than the bond dissociation energy, $\underline{D}^\circ_o$. A number of authors[2-13] have discussed this phenomenon, and the concensus is that it is a result of a non-equilibrium distribution of reactant molecules[7,12] over excited vibrational states when reaction occurs; but a quantitative, uniform account for all homonuclear diatomic molecules has not been given.[13b] In this article, we review the experimental data for all seven homonuclear diatomic molecules listed above, and we attempt to set up the <u>simplest</u> theory that, without adjustable parameters, gives approximately correct values for the rate constants $\underline{k}$ and that gives an explanation for the "low" activation energies. This "simplest" theory uses the empirical spectroscopic properties

of the reactant, the empirical transport properties of the reactant and catalyst M, and the empirical vibrational relaxation probability $\underline{P}_{10}$ for the diatomic molecule.

A firmly entrenched model in many chemists' minds is that the "activation energy" represents a "barrier" between reactants and products, and thus there is a serious conceptual problem in having the observed activation energy be far less than the endothermicity of the reaction. However, this viewpoint puts the pictorial model (barrier height) ahead of the defining relation, Eq.(3); for, after all, the "activation energy" is just a name for how the rate constant $\underline{k}$ changes with temperature. If the rate constant, for some reason, increases with temperature less rapidly than expected, then the activation energy will be less than expected. If one expects the activation energy to be at least the endothermicity of the reaction and if the rate increases with temperature less rapidly than expected because excited vibrational states of the molecules are depleted below the equilibrium value, then the activation energy, Eq.(3), will be less than the endothermicity. This effect is a particularly large one for the dissociation of diatomic molecules.

A purely formal "explanation" for low activation energies is sometimes given, as follows. If the rate constant for dissociation of a diatomic molecule depends on temperature as

$$\underline{k} = \underline{C}\ \underline{T}^{\underline{m}} \exp(-\underline{D}^{\circ}_{\underline{o}}/\underline{RT}) \tag{4}$$

then Eq.(3), the activation energy is

$$\underline{E} = \underline{D}^{\circ}_{\underline{o}} + \underline{m}\ \underline{RT} \tag{5}$$

where $\bar{T}$ is the average temperature over the range of observation. If m is negative, then the activation energy E is less than the dissociation energy D_o°. If m is regarded merely as an empirical parameter, then the invocation of Eqs.(4) and (5) is not an explanation at all, but only another description of the phenomenon.

Experimental Data

The experimental data have been reviewed recently by Troe and Wagner[14a], and our Table I is taken largely from their Table I. Lloyd [14b] has reviewed the data for fluorine and chlorine. In our Table I we give the reactant A, for foreign gas M, the temperature range, the observed activation energy E (Eqs.3), the parameter m (Eq.5), the dissociation energy D_o°, and references for experimental studies of the dissociation of homonuclear diatomic molecules.[15-46] It is readily seen that observed activation energies are far less than bond dissociation energies, and the empirical parameter m is always negative, varying from -0.4 to -4.0. Spectroscopic data, vibrational relaxation times, and hard-spheres collision cross sections (Table II) were obtained from reference books and certain articles.[47-53] Some articles[54-57] have appeared with kinetic data since Troe and Wagner's review.

General Molecular Model

The purpose of this paper is to find the simplest possible molecular model that correctly indicates the low activation energies and that utilizes no adjustable parameters. First, we present a general mechanism in terms of vibrational states of the

reactant; and next, we set up three specific models for energy-transfer and dissociative processes. The predictions of these models are then compared with experiment.

The chemical reaction of Eq.(1) is abbreviated to read

$$A + M \rightarrow \text{products}$$

The individual vibrational states A_i of the reactant are identified (omission of explicit mention of rotational and translational states implies that the reactant effectively has an equilibrium distribution over such states, and the collision constants later defined include the effect of the equilibrium range of such states). We define three different inelastic collision processes: (1) The rate of activation of A from initial state i to final state j upon collision with M is

$$R_{ij}\ (\text{up}) = a_{ij}[A_i][M] \tag{6}$$

(2) The rate of de-activation of A from initial state i to final state j is

$$R_{ij}\ (\text{down}) = b_{ij}[A_i][M] \tag{7}$$

(3) The rate of dissociation of A from state i to the continuum of free atoms is

$$R_{ic} = c_i[A_i][M] \tag{8}$$

The rate of the chemical reaction is then

$$R = -\frac{d[A]}{dt} = \sum_{i=0}^{t} c_i[A_i][M] \tag{9}$$

where t is the "top" bound state of the diatomic molecule A. The total number of reactant molecules is the sum over all vibrational states

$$[A] = \sum_{\underline{i}} [A_{\underline{i}}] \tag{10}$$

If Eq. (9) is multiplied by $[A]/\Sigma[A_{\underline{i}}]$ and terms are rearranged, we obtain

$$R = [M][A] \sum_{\underline{i}} \underline{c}_{\underline{i}} \, \underline{X}_{\underline{i}} \tag{11}$$

where $\underline{X}_{\underline{i}}$ is the mole fraction of molecules in state $\underline{i}$, $\underline{X}_{\underline{i}} = [A_{\underline{i}}]/[A]$, and the rate constant, Rate/[M][A], is expressed as $\underline{k} = \sum_{\underline{i}} \underline{c}_{\underline{i}} \underline{X}_{\underline{i}}$. This general model is illustrated for a truncated harmonic oscillator in Figure 1 and for a Morse oscillator in Figure 2.

For an equilibrium distribution over vibrational states, the mole fraction in state $\underline{i}$ is simply

$$[X_{\underline{i}}]_{eq} = (f_{\underline{v}})^{-1} \exp(-\varepsilon_{\underline{i}}/\underset{\sim}{k}\underline{T}) \tag{12}$$

where $\varepsilon_{\underline{i}}$ is the vibrational energy relative to the zero point level, $\underset{\sim}{k}$ is Boltzman's constant, and $\underline{f}_{\underline{v}}$ is the vibrational partition function. During chemical reaction we do not have an equilibrium distribution over vibrational states, and the mole fractions $\underline{X}_{\underline{i}}$ are not easily evaluated. To obtain the actual distribution over vibrational states, we need to solve the simultaneous rate equations

$$\frac{d[A_{\underline{i}}]}{dt} = [M] \sum_{\underline{j}=0}^{\underline{i}-1} \underline{a}_{\underline{j}\underline{i}} [A_{\underline{j}}] + [M] \sum_{\underline{j}=\underline{i}+1}^{\underline{t}} \underline{b}_{\underline{j}\underline{i}} [A_{\underline{j}}] \tag{13}$$

$$- [M][A_{\underline{i}}] \left\{ \sum_{\underline{j}=0}^{\underline{i}-1} \underline{b}_{\underline{i}\underline{j}} + \sum_{\underline{j}=\underline{i}+1}^{\underline{t}} \underline{a}_{\underline{i}\underline{j}} + \underline{c}_{\underline{i}} \right\}$$

with one such equation for each state $\underline{i}$ from zero to $\underline{t}$. It has been shown by detailed computations[12], that after an extremely

short induction period the relative concentrations $[A_i]/[A]$ assume a steady-state distribution, that is, these ratios do not change with time even though the reactant as a whole is rapidly disappearing and each state i decreases accordingly. Thus, as an excellent approximation

$$\frac{d([A_i]/[A])}{dt} = \frac{1}{[A]}\frac{d[A_i]}{dt} - \frac{[A_i]}{[A]^2}\frac{d[A]}{dt} \approx 0 \qquad (14)$$

Upon substitution of Eqs.(9) and (13) into Eq.(14), we obtain an expression suitable for evaluating the steady-state concentration of A_i by a method of successive approximations

$$X_i = \frac{\sum_{0}^{i-1} a_{ji}X_j + \sum_{i+1}^{t} b_{ji}X_j}{c_i + \sum_{0}^{i-1} b_{ij} + \sum_{i+1}^{t} a_{ij} - \sum_{i=0}^{t} c_i X_i} \qquad (15)$$

With a set of rate constants a_{ij}, b_{ji}, and c_i, we take as the zero approximation the equilibrium mole fractions, Eq.(12), to find a first approximation to the set of non-equilibrium mole fractions, X_i (i=0,1,2,...t). This first approximation is then substituted into the right hand side of Eq.(15) to find the second approximation to X_i, and the process can be repeated to any desired degree of convergence.

Microscopic reversibility gives a general relation between rate constants for activation and deactivation of diatomic molecules

$$a_{ij}/b_{ji} = \exp[-(\varepsilon_j - \varepsilon_i)/kT] \qquad (16)$$

The remaining problem is to set up models for the evaluation of the detailed rate constants $\underline{a}$, $\underline{b}$, and $\underline{c}$.

Three Specific Models

I. Ladder Climbing model with truncated harmonic oscillator.

This model has been used several times in the past. It uses the harmonic-oscillator conditions on light absorption or emission as restrictions on energy transfer such that activation and deactivation occur only between adjacent states

$$\underline{a}_{\underline{i}\underline{j}} = \underline{b}_{\underline{i}\underline{j}} = 0 \text{ for } \underline{j} \neq \underline{i} \pm 1 \tag{17}$$

With this restriction, we use the simplified nomenclature

$$\underline{a}_{\underline{i}} = \underline{a}_{\underline{i},\underline{i}+1};\ \underline{b}_{\underline{i}} = \underline{b}_{\underline{i},\underline{i}-1} \tag{18}$$

A further property of harmonic-oscillator spectroscopy is used to evaluate the deactivation rate constant at any level in terms of the deactivation constant between the two lowest levels

$$\underline{b}_{\underline{i}} = \underline{i}\underline{b}_1 \tag{19}$$

From microscopic reversibility, Eq.(16), and from Eq.(19), we obtain a general expression for the activation rate constants

$$\underline{a}_{\underline{i}} = (\underline{i}+1)\underline{b}_1 \exp(-\underline{h}\nu/\underline{k}T) \tag{20}$$

where $\underline{h}$ is Planck's constant and ν is the harmonic oscillator vibration frequency. The name "ladder climbing model" implies that the molecule dissociates only from the top vibrational level, $\varepsilon_{\underline{t}}$:

$$\underline{c}_{\underline{i}} = 0 \text{ for } \underline{i} < \underline{t} \tag{21}$$

The specific assumption made here is that from the top rung, the molecule dissociates upon every sufficiently energetic collision

$$\underline{c}_{\underline{t}} = \underline{Z} \exp[-(\underline{D}_o^\circ - \varepsilon_{\underline{t}})/\underset{\sim}{k}T] \tag{22}$$

where $\underline{Z}$ is the rate constant for a hard-spheres collision

$$Z = \pi\sigma^2(8\underset{\sim}{k}T/\pi\mu)^{\frac{1}{2}} \tag{23}$$

σ is the hard-spheres collision diameter (evaluated from viscosity, for example), and μ is the reduced mass between A and M.

The evaluation of the vibrational relaxation constant $\underline{b}_{10}$ or $\underline{b}_1$ is explained by two recent books.[47,48] We need this constant as a function of temperature, and a convenient form is the table and interpolation formula by Millikan and White.[49] In this way we find $\underline{b}_1$ for all diatomic molecules at all temperatures of interest, except H_2, which is not included in Millikan and White's list. The value of b, for H_2 in Ar is obtained from Kiefer and Lutz[50]. Molecular properties needed to evaluate the collision constant Z are given in Table II.

II. Truncated Harmonic Oscillator (Fig. 1).

This model is the same as I except that we accept the possibility of dissociation of the reactant from any vibrational state $\underline{i}$, instead of just the top state $\underline{t}$. From a given state $\underline{i}$, activation can occur to only one final state $\underline{i}+1$ with an energy jump of $\underline{h}\nu$; but dissociation can occur into the continuum of states with an energy jump of $(\underline{D}_o^\circ - \varepsilon_{\underline{i}})$ or more. Except for the greater jump in energy, the transition to the continuum should be more

probable than transition to the single state $\underline{i}+1$ because of the greater density of final states. It is assumed that the ratio of dissociation to activation is

$$\frac{\underline{c}_{\underline{i}}}{\underline{a}_{\underline{i}}} = \beta \frac{\exp[-(\underline{D}_{\underline{o}}^{\circ} - \underline{\varepsilon}_{\underline{i}})/\underline{k}\underline{T}]}{\exp[-h\nu/\underline{k}\underline{T}]} \tag{24}$$

where $\beta > 1$ and is the same for all states $\underline{i}$. In effect, we assume that dissociation into the continuum of final states has a larger pre-exponential factor than activation to the single, next higher state. The value of β can be found from the expression for $\underline{c}_{\underline{t}}$, Eq.(22). With β evaluated from Eq.(22) and with $\underline{a}_{\underline{i}}$ obtained from Eq.(20), we have a general expression for the dissociation rate constants

$$\underline{c}_{\underline{i}} = [(i+1)/(t+1)]\underline{Z} \exp[-(\underline{D}_{\underline{o}}^{\circ} - \underline{\varepsilon}_{\underline{i}})/\underline{k}\underline{T}] \tag{25}$$

For this model $\underline{a}_{\underline{i}}$ and $\underline{b}_{\underline{i}}$ are the same as for model I, respectively, Eq.(20) and Eq.(19).

As shown in a subsequent section, Eq.(35), at equilibrium all vibrational states contribute approximately the same amount to the decomposition rate--they differ only by the factor $(\underline{i}+1)/(\underline{t}+1)$. There are $\underline{t}+1$ approximately equal, parallel channels of reaction, some involving low lying reactants making improbable big jumps to dissociation and some involving improbable highly vibrationally excited reactants making small jumps to dissociation.

III. Morse oscillator with all transitions allowed (Fig. 2).

The vibrational energy levels for the Morse oscillator are

$$\frac{\underline{\varepsilon}_{\underline{i}}}{\underline{h}\underline{c}} = (\underline{i}+\tfrac{1}{2})\omega_e - (\underline{i}+\tfrac{1}{2})^2 \omega_e \underline{x}_e \tag{26}$$

where $\underset{\sim}{c}$ is the velocity of light, ω_e is the fundamental frequency in cm^{-1} and $\underline{x}_e$ is the anharmonicity constant. Both ω_e and $\underline{x}_e$ are readily evaluated from spectroscopic data.[52] Stevens[48] gives a model for transitions between all bound states of a Morse oscillator, which readily permits all values of deactivation constants $\underline{b}_{ij}$ to be found:

$$\underline{b}_{\underline{i}+\underline{r},\underline{i}} = \underline{b}_{10}\underline{x}_e^{\underline{r}-1}[(\underline{i}+\underline{r})!/\underline{i}!\underline{r}^2] \tag{27}$$

From microscopic reversibility, the activation constants $\underline{a}_{ij}$ are obtained

$$\underline{a}_{\underline{i},\underline{i}+\underline{r}} = \underline{b}_{10}\underline{x}_e^{\underline{r}-1}[(\underline{i}+\underline{r})!/\underline{i}!\underline{r}^2]\exp[-(\underline{D}_o^\circ-\underline{\varepsilon}_{\underline{i}})/\underline{\underline{k}}\underline{T}) \tag{28}$$

The rate constants for dissociation from any state c_i are the same for model II, Eq.(25). These constants may be factored into the collision rate constant Z and the transition probability P

$$\underline{a}_{ij} = \underline{Z}\ \underline{P}_{ij},\ \underline{b}_{ij} = \underline{Z}\ \underline{P}_{ij},\ \underline{c}_{\underline{i}} = \underline{Z}\ \underline{P}_{\underline{i}c} \tag{29}$$

For H_2 in Ar at 3000°K, the transition probability matrix $\underline{P}_{ij}$ is given in reference 1. The dissociation probability vector $\underline{P}_{\underline{i}c}$ is given in the same table. Although this model permits all transitions, large changes in vibrational quantum number are of low probability. It is interesting to note that for quantum levels above the fifth, dissociation to the dense states of the continuum is more probable than deactivation to the small number of low lying vibrational states. Above the fourth state, dissociation across many quantum states is more probable than activation to the next higher state. The density of final states is an important factor in determining transition rates.

For three models, we can evaluate all values of the energy-transfer functions $\underline{a}_{ij}$ and $\underline{b}_{ij}$ and the dissociation constants $\underline{c}_i$ from molecular properties obtained by separate experiments: $\underline{b}_{10}$, vibrational relaxation; ω and $\underline{x}_e$, Raman spectroscopy; $\underline{Z}$, viscosity or second virial coefficients. With these constants we evaluate the vibrational distribution function by successive approximations from Eq.(15), the rate constants from Eq.(11), and the activation energy from Eq.(3). In the next sections we test the predictions of $\underline{E}$ and $\underline{k}$ by the three models, first for the hypothetical situation of reactant with an equilibrium distribution over vibrational states and next for non-equilibrium, steady-state, relative distribution functions.

Model Predictions if Reactants Have Equilibrium Distribution Function

For rate expression, we go back to Eq.(9), $\Sigma \underline{c}_i [A_i][M]$. Using Eq.(12) for the equilibrium concentration of reactant in the vibrational state $\underline{i}$, we obtain

$$\underline{k}_{eq} = (f_v)^{-1} \sum_{\underline{i}} \underline{c}_i \exp(-\varepsilon_i/\underline{k}\underline{T}) \qquad (30)$$

For model I, there is only one term in the sum, since $\underline{c_i}$ is assumed to be zero for all states except the top one $\underline{t}$

$$\underline{k}^{I}_{eq} = (Z/f_v) \exp[-(\underline{D}^\circ_o - \varepsilon_{\underline{t}})/\underset{\sim}{k}\underline{T}] \exp[-\varepsilon_{\underline{t}}/\underset{\sim}{k}\underline{T}] \tag{31}$$

$$= (Z/f_v) \exp[-\underline{D}^\circ_o/\underset{\sim}{k}\underline{T}] \tag{32}$$

For models II and III the rate constant expression is

$$\underline{k}_{eq} = (Z/f_v) \sum_i \frac{i+1}{t+1} \exp[-(\underline{D}^\circ_o - \varepsilon_i)/\underset{\sim}{k}\underline{T}] \exp[-\varepsilon_i/\underset{\sim}{k}\underline{T}] \tag{33}$$

$$= (Z/f_v) \exp[-\underline{D}^\circ_o/\underset{\sim}{k}\underline{T}] \sum_{i=0}^{t} \frac{i+1}{t+1} \tag{34}$$

$$= (Z/f_v) \exp[-\underline{D}^\circ_o/\underset{\sim}{k}\underline{T}] \left(\frac{t+2}{2}\right) \tag{35}$$

Thus the temperature dependence of all three models is the same if there is an equilibrium distribution over vibrational states

$$E_{eq} = D^\circ_o - R \frac{d \ln Z}{d(1/T)} + R \frac{d \ln f_v}{d(1/T)} \tag{36}$$

For the harmonic oscillators, models I and II, the vibrational partition function is approximately $(1 - e^{-h\nu/\underset{\sim}{k}\underline{T}})^{-1}$, its temperature derivative in Eq.(36) varies between 0 at low temperature and $\underline{RT}$ at high temperature. If the collision rate constant varies as $T^{\frac{1}{2}}$, Eq.(23), its contribution to the activation energy is $\frac{1}{2}$ $\underline{RT}$. Thus these two models predict

$$\underline{D}^\circ_o - \tfrac{1}{2}\ \underline{RT} \leq \underline{E}_{eq} \leq \underline{D}^\circ_o + \tfrac{1}{2}\ \underline{RT} \tag{37}$$

High $\underline{T}$ Low $\underline{T}$

The observed activation energies in Table I differ from $\underline{D}^\circ_o$ substantially more than the limits given by Eq.(37). Thus these

models are inadequate to explain the observed activation energies if the vibrational states have an equilibrium distribution. Similar conclusions apply to model III if the quantities are evaluated numerically.

Calculated Activation Energies and Rate Constants with Non-Equilibrium Distribution Function

Hydrogen--By use of the values of the transition constants for activation, deactivation, and dissociation, rate constants and activation energies for the dissociation of H_2 in a heat bath of Ar were calculated each 400° between 1000° and 5000°K. For each of the three models, the results are given in Table III. It is readily apparent that the ladder-climbing model gives activation energies that vary with temperature in a manner quite different from that observed. At low temperatures, this model greatly underestimates the rate. At high temperatures where vibrational energy transfer becomes fast, the rate constants are less than those calculated by the other models, but the difference is much less than that found at low temperatures. This partial "catching-up" at high temperatures causes the rate to increase faster than expected at high temperatures, and the activation energy greatly exceeds the dissociation energy. The other models, which permit dissociation from all vibrational states, show activation energies that decrease with temperature, in the same general sense as that observed.

The calculated and observed rate constants for H_2 are compared in Figure 3. Calculated curves are given for model I and model III.

The experimental data show substantial disagreement between different investigators. Even so, the rate constants for model I are well below the experimental data, and those for model III are in reasonably good agreement with the data. On the basis of these results, model I is dropped from further consideration.

Fluorine--Fluorine is relatively insensitive to trace impurities, whereas H_2 and Cl_2 are susceptible to traces of O_2 (H_2 being attacked by O or HO; Cl_2 dissociating by way of ClOO and ClO[58]). Thus, fluorine was chosen for the most intensive calculations, and in particular for comparisons of model II and model III.

The equilibrium and non-equilibrium distribution of F_2 over vibrational states are given in reference 1 in terms of the full Morse calculation (model III). The logarithm of mole fraction X_i is given as a function of vibrational energy for 500, 1000, and 2500°K. At 500°K, the steady-state distribution is very close to the equilibrium distribution up to the 17th quantum state, and then it rapidly falls off at higher states. At 1000°K, the fall-off begins at about state 11. At 2500°K there is serious depletion of excited vibrational states above the third or fourth level. Reference 1 also gives the dissociation rate constants c_i as a function of quantum state and temperature. At very high quantum numbers, the constants c_i differ only slightly between 500, 1000, and 2500°K. At low quantum numbers there is a great spread with temperature in c_i at a given state i. The relative "distribution function for molecules that react" is given by the product of mole fractions X_i and dissociation constant c_i, and these are given

for three temperatures as Figure 4. At 500°K, the contribution to reaction is almost uniform from states 2 to 20, with a slight drop off at low quantum numbers (see Eq.25) and a large drop off at high quantum numbers from non-equilibrium. At 1000°K the reacting states are equally important from about 2 to 15. At 2500°K the states that react lie largely between 0 and 7, with a fairly fast fall-off above the seventh state. Figure 4 explains why the activation energy decreases with increasing temperature: With an equilibrium distribution all 29 states react equally except for the factor $(\underline{i}+1)/(\underline{t}+1)$, Eq.(25), and thus there are 29 parallel reaction channels. At 500°K the decomposition reaction has set up a steady-state distribution such that upper states are depleted. The depletion of a given state $\underline{i}$ is caused both by the rapid loss of $\underline{i}$ states to atoms and by state $\underline{i}$ being skipped as lower states go directly to atoms. From Figure 4, we see that at 500°K there are only about 20 effective reaction channels; at 1000°K the number is about 15; and at 2500°K the number is about 7. This decrease in "number of states that react" by virtue of the non-equilibrium distribution at high energies causes the rate constant to increase with temperature less rapidly than expected, and thus the activation energy is lower than expected (see Eq.3).

The observed rate constants for F_2 are shown in Figure 5 with curves calculated by model II and model III. These two models agree fairly well with the data, and they agree so closely with each other that the simpler model II is selected for all further comparisons.

All other cases--By use of the truncated harmonic oscillator model (Fig. 1 and model II), the activation energies as a function of temperature were calculated for all four halogens, N_2 and O_2; and the data are given in Table IV. The calculated activation energies decrease strongly with temperature in all cases. These calculations were extended to cover the range of observed temperatures for the various cases in Table I. The last column in that table gives activation energies calculated by means of the truncated harmonic oscillator, model II. Within the experimental uncertainty of the data, the calculated activation energies agree very well with those observed.

Observed rate constants for I_2, N_2, and O_2 are plotted in Figure 6A,B, and C. Two calculated curves are given on each figure, each is based on model II. The upper curve is calculated on the basis of an equilibrium distribution over vibrational states, and the lower curve is based on the non-equilibrium distribution. The data for I_2, N_2, and even O_2 are fairly well defined and show adequate agreement between different investigators. In these cases the non-equilibrium curve calculated from model II agrees fairly well with the observed points, and the equilibrium curve lies well above the data. The data for Br_2 and especially Cl_2 show strong disagreements between different investigators (perhaps due to participation of small amounts of O_2 impurities as catalyst via ClOO and ClO[58]). The data for Cl_2 and Br_2 show so much experimental error that it is not useful to speak of agreement or non-agreement between calculated and observed rate constants. However, our calculated non-equilibrium

rates agree rather well with the line for Cl_2 as recommended by Lloyd.[14b]

The data for O_2 cover a wider range of temperature than any other, up to 18,000°K. The calculated non-equilibrium curve shows an increase in activation energy at extremely high temperatures (all other cases show this same effect at temperatures well above the range of observations). The experimental data for O_2 do not show this effect, but it would be difficult to extract it from the data since it appears only above 10,000°K. The explanation of this effect can be seen by examination and extension of the distribution function for molecules that react in Fig. 4. At the highest temperature shown there, the states that react are the bottom 6 or 7. At even higher temperatures it may be expected that this function will be narrowed to the lowest one or two states. Then the only reaction is the strong collision channel from the ground state to the continuum, for which single process there is an energy barrier of $\underline{D}_o^\circ$. The rate can no longer abstain from increasing "as expected" because the number of states that react cannot shrink below one (This ultimate increase of activation energy at very high temperature might be observed with F_2).

The Reverse Reaction

These calculations all refer to the forward reaction or dissociation of the diatomic molecule, Eq.(1), and no account has been given to the reverse process or the recombination reaction. As atoms accumulate and recombination occurs, the population of highly excited vibrational states will surely change in the

direction of increased occupancy. There are many upper vibrational states for which a collision is more likely to give re-dissociation than deactivation. This fact is of importance to the theory of recombination of atoms. Some theories of recombination regard that process as complete when the atom pair is deactivated below the dissociation limit, $\underline{D}_0^\circ$. However, the highly excited vibrational states of X_2 are, in effect, closer to products than to reactant. The negative activation energy for atom recombination arises, in part, from the redissociation of highly excited X_2, an effect that increases with increasing temperature, Figure 4.

A complete theory of the dissociation of diatomic molecules should explicitly consider rotational motions and excited electronic states of the diatomic molecules. This presentation, however, shows that non-equilibrium distributions of the vibrational states of the ground electronic states are sufficient to explain the low, observed, activation energies.

Summary

The observed activation energy for the dissociation of diatomic molecules is substantially less than the bond dissociation energy, and it decreases with increasing temperature. This effect cannot be explained by a ladder-climbing model of the reaction process with dissociation occurring only from the top vibrational level, even with allowance for a non-equilibrium distribution over vibrational states. This effect is readily explained by several models that allow dissociation to occur from any and all vibrational states and with allowance for non-equilibrium

distribution over vibrational states. Two such models were set up that permitted the calculation of dissociation rate constants from separately determined vibrational relaxation times, vibrational frequency, and hard-spheres collision cross section--with no adjustable parameters. The non-equilibrium versions of these models give satisfactory predictions of rate constants and a good account of the observed low activation energies. These calculations indicate that diatomic molecules dissociate from all vibrational states.

Acknowledgement

This work was supported by the U.S. Atomic Energy Commission through the Inorganic Materials Research Division, Lawrence Radiation Laboratory, Berkeley, California.

Table I. Experimental Data on Activation Energies for the Dissociation of Homonuclear Diatomic Molecules.

A	M	T	D°_o kcal	E_{obs} kcal	m Eq.5	Ref.	$E_{calc.}$ Model II
F_2	Ar	1300-1600	37.1	30±4	-2.5	15	31.7
	Ne	1650-2700		24±5	-3.0	16	30.3
	Ar	1300-1600		27.3±2.5	-3.4	17	31.7
	Xe	1300-1600		31.1	-2.1	17	31.7
Cl_2	Ar	1700-2500	57.0	48.3	-2.1	18	48.4
		1600-2600		50	-1.7	19	49.9
		1700-2600		41±5	-4.0	20	48.6
		1600-2600		45±2	-2.9	21	49.9
		1700-2600		48.3	-2.0	22	48.2
Br_2	Ar	1300-1900	45.5	41.4	-1.3	23	39.7
		1400-2700		41.4	-1.0	24	38.5
		1200-2200		32.4	-3.8	25	40.3
I_2	Ar	1000-1600	35.6	29.7	-2.3	26,27	31.6
		850-1650		30.4	-2.1	28	31.9
O_2	Ar	5000-18000	118.0	110	-0.4	29,30	102.7
		3800-5000		106±5	-1.4	31,32	99.1
		4000-6000		108	-1.0	33	97.5
		3400-7500		108	-1.2	34	97.7
		3000-5000		114	-0.5	35	103.7
	O_2	3000-5000		98	-2.5	29,36	
		4000-7000		91	-2.5	37	96.4
		2500-4000		108	-1.5	35	108.2
		3000-6000		109±5	-1.0	32	102.0
		2600-7000		85	-3.7	38	103.3

Table I Cont'd.

A	M	T	D°_{o} kcal	E_{obs} kcal	m Eq. 5	Ref.	$E_{calc.}$ Model II
H_2	Ar	2800-4500	103.3	97	-0.9	39	88.7
		3000-5300		97	-0.8	40	86.2
		2800-5000		97	-0.8	41	87.7
		2290-3790		97	-1.0	42	95.4
	Xe	3000-4500		100	-0.4	43	
	H_2	3000-4500		92	-1.5	43	
	H	3000-4500		100	-0.4	43	
D_2	Ar	3000-4800	105	97	-1.0	39	
	Ar	3000-4900		97	-1.0	44	
N_2	Ar	6000-9000	225	218	-0.5	45	195.4
		6000-10000		204	-1.3	46	193.9
	N_2	6000-9000		218	-0.5	45	195.4
		6000-10000		198	-1.7	46	193.9
	N	6000-9000		203	-1.5	45	

Table II. Molecular Properties Used to Evaluate Vibrational Relaxation Constant $b_1(T)$ and Hard-Spheres Collision Constant z.

A	M	ω_e cm^{-1}	$\omega_e x_e$	t+1 no. of states	D_o° kcal/mole	ε/k °K of A	r_o A	A of Ref. 49
H_2	Ar	4395	126.2	14	103.3	38	2.93	-
H_2	Ar	4395	0	8	103.3	38	2.93	-
F_2	F_2	892	14.8	29	37.1	112	3.65	65
F_2	F_2	892	0	15	37.1	112	3.65	65
Cl_2	Cl_2	557	0	36	57.1	257	4.40	58
Br_2	Br_2	321	0	50	45.5	520	4.27	48
I_2	I_2	213	0	58	35.5	550	4.98	29
N_2	N_2	2331	0	33	225	91.5	3.68	220
O_2	Ar	1554	0	27	118	113	3.43	129
O_2	O_2	1554	0	27	118	113	3.43	165
Ref.		52				51	51	49

Table III. Dissociation of Hydrogen by Argon. Calculated Activation Energies for Three Models

T °K	Ladder climbing I	Harmonic oscillator II	Morse function III
1000	95.5	103.5	103.5
1400	97.0	102.9	102.1
1800	98.5	101.8	100.7
2200	99.8	99.8	98.6
2600	101.1	96.9	95.6
3000	102.3	92.8	91.7
3400	103.5	88.4	87.4
3800	104.6	85.0	83.9
4200	105.7	83.7	82.0
4600	106.8	84.6	81.9
5000			

Table IV. Calculated Activation Energies (kilocalories) from the Truncated Harmonic Oscillator Model II.

T °K	N_2	O_2	F_2	Cl_2	Br_2	I_2
500	225	118	36	56	44	34
1000	224	117	33	54	42	32
1500	224	115	30	52	40	29
2000	222	114	30	48	36	26
2500	222	110	29	46	35	26
3000	220	109				
3500	220	103				
4000	217	101				
4500	214	98				
5000	209	94				
5500	206	94				
6000	204	92				
6500	197	93				
7000	197	92				
7500	189	96				
8000						

Appendix A.

Table A-I. Transition Probabilities Per Collision for H_2 With Ar at 3000°K.

i	0	1	2	3	4	5	6	7	8	9	10	11	12	13
j P_{ij}														
0		.14E-04	.42E-06	.35E-07	.55E-08	.12E-08	.37E-09	.14E-09	.61E-10	.32E-10	.19E-10	.13E-10	.98E-11	.82E-11
1	.20E-05		.58E-04	.28E-05	.34E-06	.67E-07	.18E-07	.65E-08	.28E-08	.14E-08	.83E-09	.55E-09	.41E-09	.33E-09
2	.88E-08	.90E-05		.98E-04	.67E-05	.10E-05	.25E-06	.81E-07	.33E-07	.16E-07	.91E-08	.59E-08	.43E-08	.35E-08
3	.13E-09	.76E-07	.17E-04		.14E-03	.12E-04	.23E-05	.65E-06	.25E-06	.11E-06	.61E-07	.39E-07	.27E-07	.22E-07
4	.40E-11	.18E-08	.23E-06	.27E-04		.18E-03	.19E-04	.43E-05	.14E-05	.60E-06	.31E-06	.18E-06	.13E-06	.98E-07
5	.12E-12	.80E-10	.80E-08	.53E-06	.39E-04		.22E-03	.27E-04	.71E-05	.27E-05	.13E-05	.72E-06	.47E-06	.35E-06
6	.15E-13	.55E-11	.48E-09	.25E-07	.11E-05	.54E-04		.26E-03	.37E-04	.11E-04	.46E-05	.24E-05	.15E-05	.11E-05
7	.16E-14	.55E-12	.44E-10	.20E-08	.68E-07	.20E-05	.73E-04		.30E-03	.49E-04	.16E-04	.74E-05	.47E-05	.29E-05
8	.23E-15	.75E-13	.58E-11	.25E-09	.71E-08	.16E-06	.34E-05	.95E-04		.33E-03	.62E-04	.23E-04	.11E-04	.71E-05
9	.43E-16	.14E-13	.11E-11	.41E-10	.11E-08	.22E-07	.36E-06	.57E-05	.12E-03		.37E-03	.77E-04	.31E-04	.17E-04
10	.11E-16	.33E-14	.23E-12	.90E-11	.23E-09	.42E-08	.61E-07	.76E-06	.91E-05	.15E-03		.41E-03	.93E-04	.40E-04
11	.33E-17	.10E-14	.70E-13	.26E-11	.64E-10	.11E-08	.15E-07	.16E-06	.15E-05	.14E-04	.19E-03		.45E-03	.11E-03
12	.13E-17	.39E-15	.26E-13	.96E-12	.23E-10	.38E-09	.48E-08	.48E-07	.40E-06	.30E-05	.22E-04	.24E-03		.49E-03
13	.62E-18	.19E-15	.12E-13	.45E-12	.10E-10	.17E-09	.20E-08	.19E-07	.15E-06	.96E-06	.56E-05	.34E-04	.29E-03	
P_{ic}	.40E-08	.44E-07	.38E-06	.27E-05	.16E-04	.86E-04	.39E-03	.15E-02	.54E-02	.16E-01	.44E-01	.10	.21	.39

P_{ij}--transition probability from vibrational state i to state j.

P_{ic}--transition probability from vibrational state i to continuum of dissociated atoms.

Table A-II. Mole Fractions in Various Vibrational States and the Dissociation Rate Constant for Vibrational States of Fluorine as a Function of Temperature.

Quantum number, i	Energy cm^{-1}	500°K			1000°K			2500°K		
		$\log X_{i,eq}$	$\log X_i$	$\log c_i$	$\log X_{i,eq}$	$\log X_i$	$\log c_i$	$\log X_{i,eq}$	$\log X_i$	$\log c_i$
0	442	-0.04	-0.04	-26.92	-0.15	-0.15	-18.72	-0.44	-0.30	-13.71
1	1305	-1.12	-1.12	-25.67	-0.69	-0.69	-18.00	-0.65	-0.59	-13.32
2	2138	-2.16	-2.16	-24.50	-1.21	-1.21	-17.36	-0.85	-0.89	-12.98
3	2941	-3.16	-3.16	-23.40	-1.71	-1.71	-16.76	-1.06	-1.22	-12.69
4	3714	-4.13	-4.13	-22.35	-2.20	-2.20	-16.20	-1.25	-1.56	-12.41
5	4458	-5.06	-5.06	-21.36	-2.67	-2.67	-15.66	-1.43	-1.92	-12.16
6	5173	-5.95	-5.95	-20.41	-3.11	-3.12	-15.16	-1.62	-2.32	-11.92
7	5858	-6.81	-6.81	-19.50	-3.54	-3.56	-14.68	-1.79	-2.75	-11.70
8	6513	-7.62	-7.62	-18.63	-3.95	-3.99	-14.23	-1.95	-3.22	-11.49
9	7138	-8.41	-8.41	-17.81	-3.33	-4.42	-13.79	-2.10	-3.74	-11.30
10	7734	-9.15	-9.15	-17.03	-4.71	-4.87	-13.38	-2.26	-4.32	-11.11
11	8301	-9.86	-9.86	-16.29	-5.06	-5.34	-12.99	-2.39	-4.94	-10.93
12	8838	-10.53	-10.84	-15.58	-5.39	-5.86	-12.63	-2.53	-5.62	-10.77
13	9345	-11.16	-11.18	-14.92	-5.71	-6.46	-12.28	-2.66	-6.35	-10.61
14	9822	-11.76	-11.82	-14.29	-6.01	-7.16	-11.95	-2.77	-7.12	-10.46
15	10270	-12.32	-12.48	-13.71	-6.29	-7.98	-11.65	-2.89	-7.94	-10.32
16	10689	-12.84	-13.22	-13.16	-6.56	-8.93	-11.36	-2.99	-8.78	-10.19
17	11078	-13.33	-14.12	-12.63	-6.80	-9.98	-11.09	-3.09	-9.63	-10.07
18	11437	-13.78	-15.24	-12.18	-7.02	-11.10	-10.85	-3.18	-10.48	-9.96
19	11766	-14.19	-16.58	-11.75	-7.22	-12.23	-10.62	-3.26	-11.32	-9.86
20	12066	-14.56	-18.03	-11.35	-7.41	-13.33	-10.41	-3.33	-12.12	-9.76
21	12337	-14.90	-19.46	-10.90	-7.58	-14.35	-10.22	-3.40	-12.89	-9.68
22	12578	-15.20	-20.77	-10.67	-7.73	-15.28	-10.06	-3.47	-13.61	-9.66
23	12789	-15.47	-21.94	-10.39	-7.87	-16.13	-9.91	-3.52	-14.28	-9.53
24	12970	-15.70	-22.97	-10.15	-7.98	-16.90	-9.78	-3.56	-14.90	-9.46
25	13122	-15.89	-23.88	-9.94	-8.07	-17.59	-9.66	-3.60	-15.48	-9.41
26	13245	-16.04	-24.68	-9.77	-8.15	-18.22	-9.57	-3.63	-16.02	-9.36
27	13338	-16.15	-25.37	-9.64	-8.21	-18.79	-9.50	-3.65	-16.51	-9.32
28	13401	-16.23	-25.96	-9.55	-8.25	-19.29	-9.44	-3.67	-16.96	-9.29

References

1. This article, without appendix A, is being published in Accounts of Chemical Research. Appendix A contains additional tables and figures.
2. O.K. Rice, J. Chem. Phys. 9, 259 (1941); 21, 750 (1953); J. Phys. Chem. 67, 6 (1962).
3. G. Careri, J. Chem. Phys. 21, 749 (1953).
4. S.K. Kim, J. Chem. Phys. 28, 1057 (1958).
5. K.E. Shuler, J. Chem. Phys. 31, 1375 (1959).
6. E.E. Nikitin and N.D. Sokolov, J. Chem. Phys. 31, 1371 (1959).
7. H.O. Pritchard, J. Phys. Chem. 65, 504 (1961).
8. S.W. Benson and T. Fueno, J. Chem. Phys. 36, 1597 (1962).
9. B. Widom, J. Chem. Phys. 34, 2050 (1961).
10. P.V. Marrone and C.E. Treanor, J. Phys. Fluids 6, 1215 (1963).
11. W.G. Valance and E.W. Schlag, J. Chem. Phys. 45, 216, 4280 (1966).
12. D.G. Rush and H.O. Pritchard, International Symposium on Combustion XI, 13 (1966).
13. a. V.H. Shui, J.P. Appleton, and J.C. Keck, J. Chem. Phys. 53, 2547 (1970).
    b. M. Warshay, J. Chem. Phys. 54, 4060 (1971).
14. a. J. Troe and H. Gg. Wagner, Ber. Bunsengesellshaft 71, 930 (1967).
    b. A.C. Lloyd, Int. J. Chem. Kin. 3, 39 (1971).
15. C.D. Johnson and D. Britton, J. Phys. Chem. 68, 3032 (1964).
16. R.W. Diesen, J. Chem. Phys. 44, 3662 (1966).
17. D.J. Seery and D. Britton, J. Phys. Chem. 70, 4074 (1966).
18. T.A. Jacobs and R.R. Giedt, J. Chem. Phys. 39, 749 (1963).
19. H. Hiraoka and R. Hardwick, J. Chem. Phys. 36, 1715 (1962).
20. R.W. Diesen and W.J. Felmlee, J. Chem. Phys. 39, 2115 (1963).
21. M. van Thiel, D.J. Seery, and D. Britton, J. Phys. Chem. 69, 834 (1965)

22. R.A. Carabetta and H.B. Palmer, J. Chem. Phys. 46, 1333 (1967).

23. D. Britton, J. Phys. Chem. 64, 742 (1960).

24. D. Britton and N. Davidson, J. Chem. Phys. 25, 810 (1956).

25. H.B. Palmer and D.F. Hornig, J. Chem. Phys. 26, 98 (1957).

26. D. Britton, N. Davidson, W. Gehman, and G. Schott, J. Chem. Phys. 25, 804 (1956).

27. D. Britton, N. Davidson, and G. Schott, Disc. Faraday Soc. 17, 58 (1954).

28. J. Troe and H.Gg. Wagner, Z physik. Chem. N.F. 55, 326 (1967).

29. H.S. Johnston, "Gas Phase Kinetics of Neutral Oxygen Species" National Standard Reference Data Series, National Bureau of Standards, Volume 20 (1968).

30. K.L. Wray, International Symposium on Combustion, X, 523 (1965); J. Chem. Phys. 37, 1254 (1962); 38, 1518 (1963).

31. J.P. Rink, J. Chem. Phys. 36, 572 (1962).

32. J.P. Rink, H. Knight, and R. Duff, J. Chem. Phys. 34, 1942 (1961).

33. O.L. Anderson, United Aircraft Corporation Research Laboratory, Report R-1828-1 (1961).

34. M. Camac and A. Vaughn, J. Chem. Phys. 34, 460 (1961).

35. S.R. Byron, J. Chem. Phys. 34, 460 (1961).

36. D.L. Matthews, Physics Fluids 2, 170 (1959).

37. S.A. Losev and N.A. Generalov, Soviet Physics, Doklady 6, 1081 (1962).

38. N.A. Generalov and S.A. Losev, J. Quant. Spect. Rad. Transfer 6, 101 (1966).

39. E.A. Sutton, J. Chem. Phys. 36, 2923 (1962).

40. R.W. Patch, J. Chem. Phys. 36, 1919 (1962).

41. J.P. Rink, J. Chem. Phys. 36, 262 (1962).

42. A.L. Myerson and W.S. Watt, J. Chem. Phys. 49, 425 (1968).

43. W.C. Gardiner and G.B. Kistiakowsky, J. Chem. Phys. 35, 1765 (1961).

44. J.P. Rink, J. Chem. Phys. 36, 1398 (1962).

45. S.R. Byron, J. Chem. Phys. 44, 1378 (1966).

46. B. Cary, Physics Fluids 8, 26 (1965).

47. T.L. Cottrell and C. McCoubry, "Molecular Energy Transfer in Gases" Butterworths, London (1961), p. 77.

48. Brian Stevens, "Collisional Activation in Gases" Pergamon Press, New York (1967), p. 39.

49. R.C. Millikan and D.R. White, J. Chem. Phys. 39, 3209 (1963).

50. J.H. Kiefer and R.W. Lutz, J. Chem. Phys. 44, 668 (1966).

51. J.O. Hirschfelder, C.F. Curtiss, and R.B. Bird, "Molecular Theory of Gases and Liquids" Wiley, New York (1954).

52. Gerhard Herzfeld, "Spectra of Diatomic Molecules" Von Nostrand, New York (1950).

53. R.C. Herman and K.E. Shuler, J. Chem. Phys. 16, 373 (1953).

54. R.W. Diesen, J. Phys. Chem. 72, 108 (1968).

55. R.K. Boyd, J.D. Brown, G. Burns, J.H. Lippiatt, J. Chem. Phys. 49, 3822 (1968).

56. R.K. Boyd, G. Burns, T.R. Lawrence, J.H. Lippiatt, J. Chem. Phys. 49, 3804 (1968).

57. J.P. Appleton, M. Steinberg, and D.J. Liquornik, J. Chem. Phys. 48, 599 (1968).

58. H.S. Johnston, E.D. Morris, Jr., and J. Van der Bogaerde, J. Am. Chem. Soc. 91, 7712 (1969).

Titles to Figures

Fig. 1. Truncated Harmonic Oscillator Model for Decomposition of Diatomic Molecule. For model I all c are assumed to be zero except c_t. For model II all c_i are allowed to be non-zero, Eq.(25). In each model only nearest neighbor transitions are considered for vibrational energy transfer.

Fig. 2. Morse Function Model for Decomposition of Diatomic Molecule. Model III considers all vibrational energy transfers and allows all states to dissociate to the continuum, Eq.(25).

Fig. 3. Dissociation of H_2 by Ar. Calculated, models I and III, and observed rate constants as a function of temperature. a. Ref. 39 (Sutton), b. Ref. 40 (Patch), c. Ref. 41 (Rink), d. Ref. 43 where M is Xe (Ref. 41 reported Ar and Xe to have same efficiency in dissociating H_2). Data points are those read from graph of Ref. 42.

Fig. 4. Distribution function for molecules that react for the vibrational states of F_2 with the Morse model III. ---- equilibrium distribution; —— non-equilibrium distribution. Note the shrinking number of states that contribute to reaction as one goes to high temperatures.

Fig. 5. Dissociation of Fluorine. Calculated curves: models II and III. Calculation based on F_2 as M. Observed data: O, with Ar, ref. 15, points taken from graph; ●, with N_e, ref. 16; □, with N_e, ref. 54, points taken from graph.

Fig. 6. Dissociation of Homonuclear Diatomic Molecules. Calculated curves are based on model II, truncated harmonic oscillator, all transitions to continuum allowed (compare Fig. 1). The lower curve is based on steady-state, non-equilibrium distribution function. The upper curve is based on the same model with the equilibrium distribution over vibrational states. Experimental points are taken from tables or read from graphs in the articles cited. k in units of cc/particle-sec.

A. I_2. O, with Ar, ref. 26, read from graph; ●, with Ar, ref. 27, read from graph (an error of a factor of 10 appears in the graph of ref. 27, and this has been corrected).

B. N_2. ●, with Ar, ref. 57, points read from graph.

C. O_2. All data in excess Ar. Points as read from graphs listed in ref. 29. □, ref. 34; O, ref. 30; ◆, ref. 108 in ref. 29; ●, ref. 33.

Titles to Appendix A Figures

Figure A-1. Br_2. □, with Ar, ref. 25; ■, Br_2 is M, ref. 25; ♦, with Ar, ref. 19; ◊, with Ar, ref. 55; ●, with Ar, ref. 56.

Figure A-2. Cl_2. □, with Ar, ref. 19; O, with Ar, ref. 18; ●, with Ar, ref. 20; ■, 5% Cl_2 in Ar, ♦, 10% Cl_2 in Ar, ref. 21; ◊, with Ar, ref. 22.

Figure A-3. Detailed distributions of mole fractions (here written as N_i) and rate constants c_i, as a function of vibrational energy.

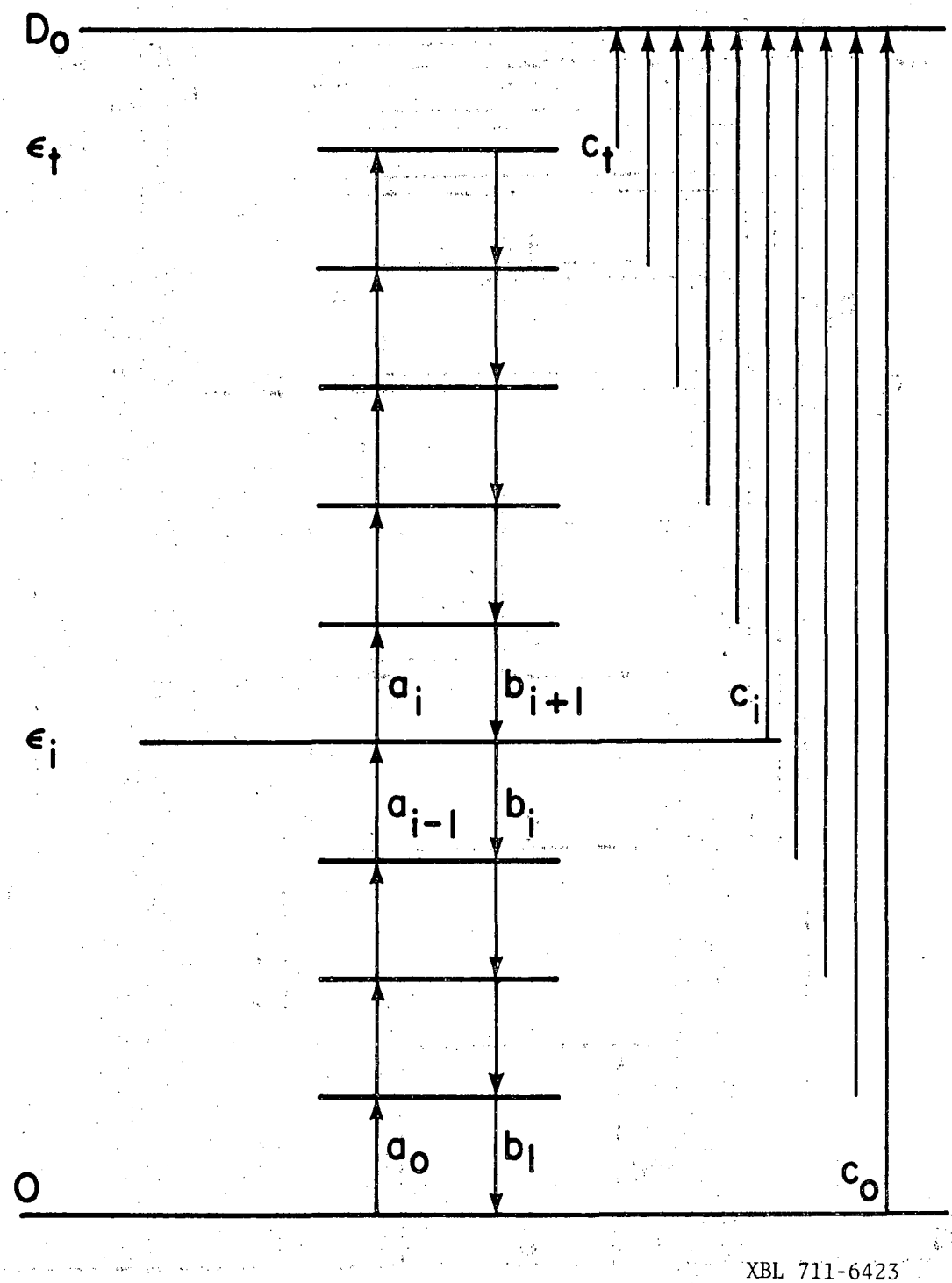

Fig. 1

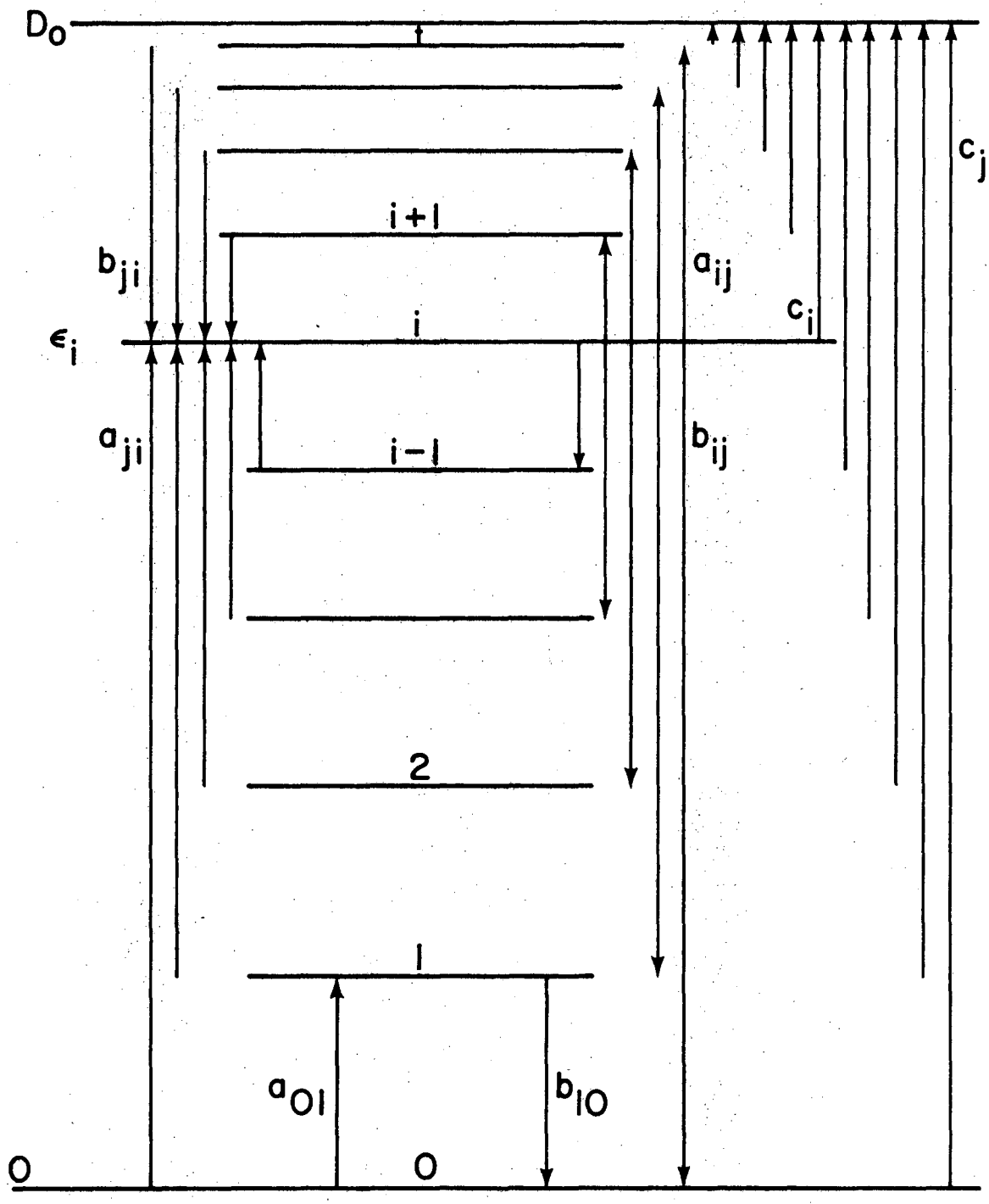

XBL 711-6424

Fig. 2

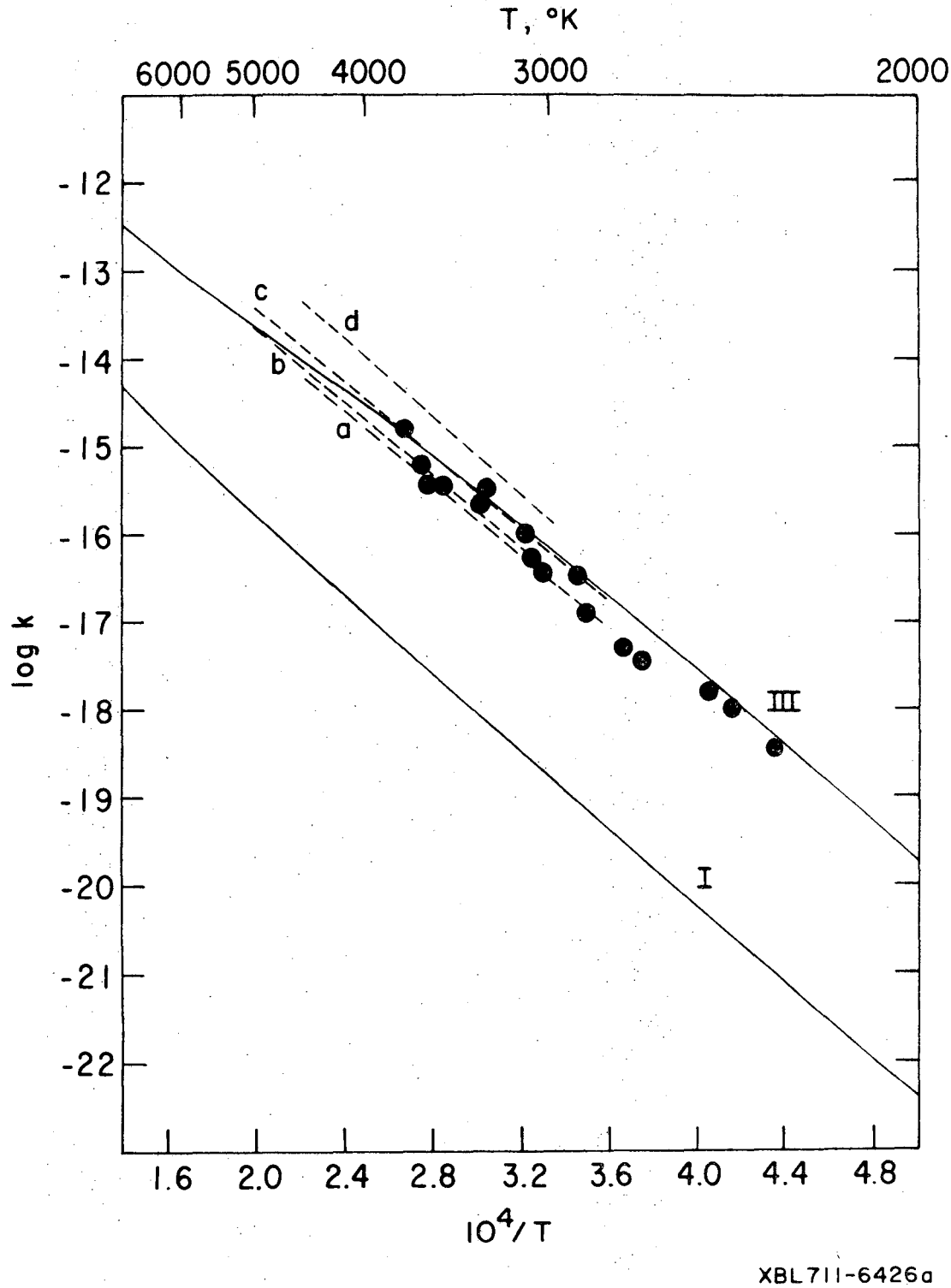
T, °K
6000 5000 4000 3000 2000
-12
-13
-14
-15
-16
-17
-18
-19
-20
-21
-22
log k
c
d
b
a
III
I
1.6 2.0 2.4 2.8 3.2 3.6 4.0 4.4 4.8
10^4/T
XBL711-6426a

Fig. 3

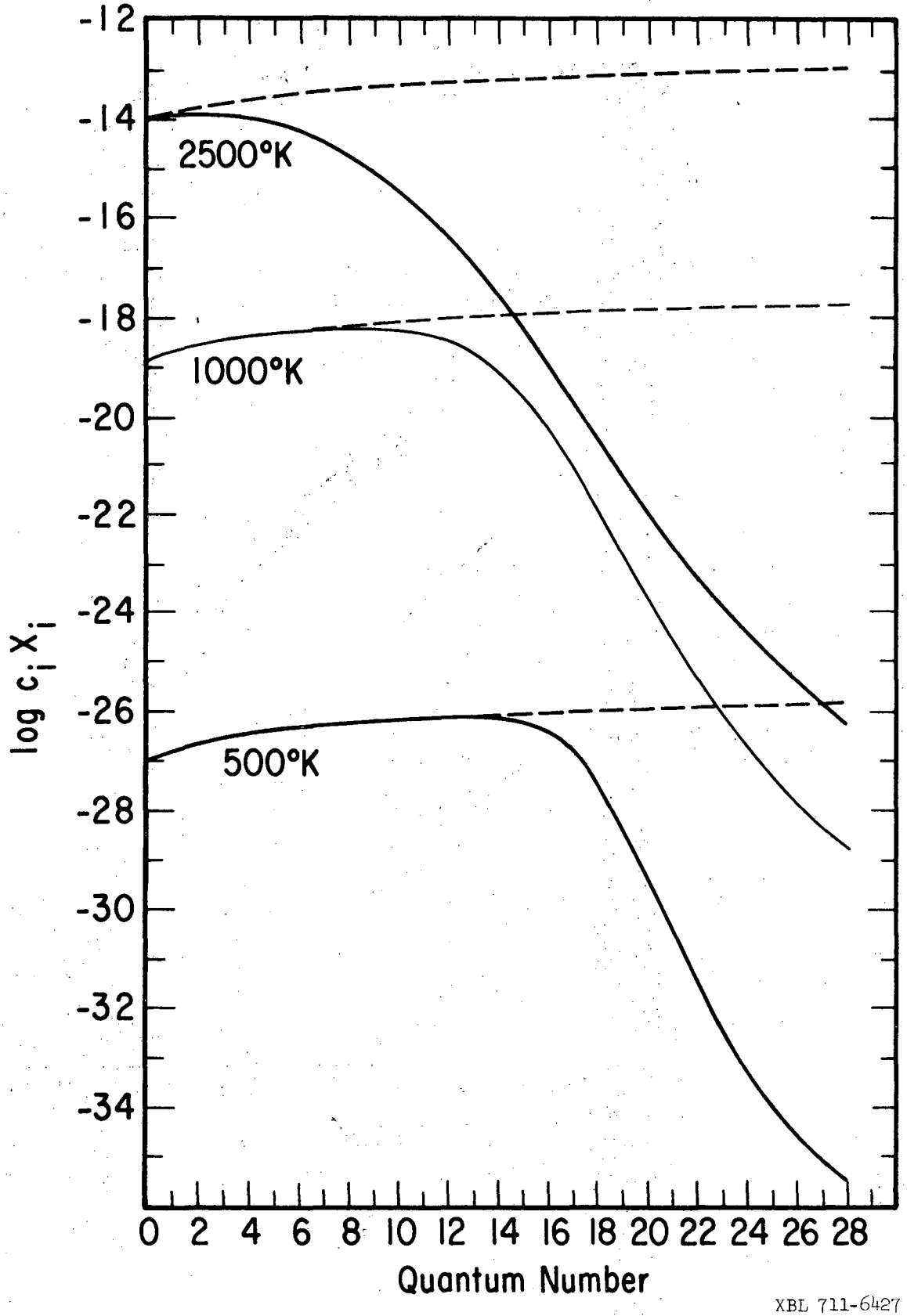
-12
-14
-16
-18
-20
-22
-24
-26
-28
-30
-32
-34
2500°K
1000°K
500°K
log $c_i X_i$
0 2 4 6 8 10 12 14 16 18 20 22 24 26 28
Quantum Number
XBL 711-6427

Fig. 4

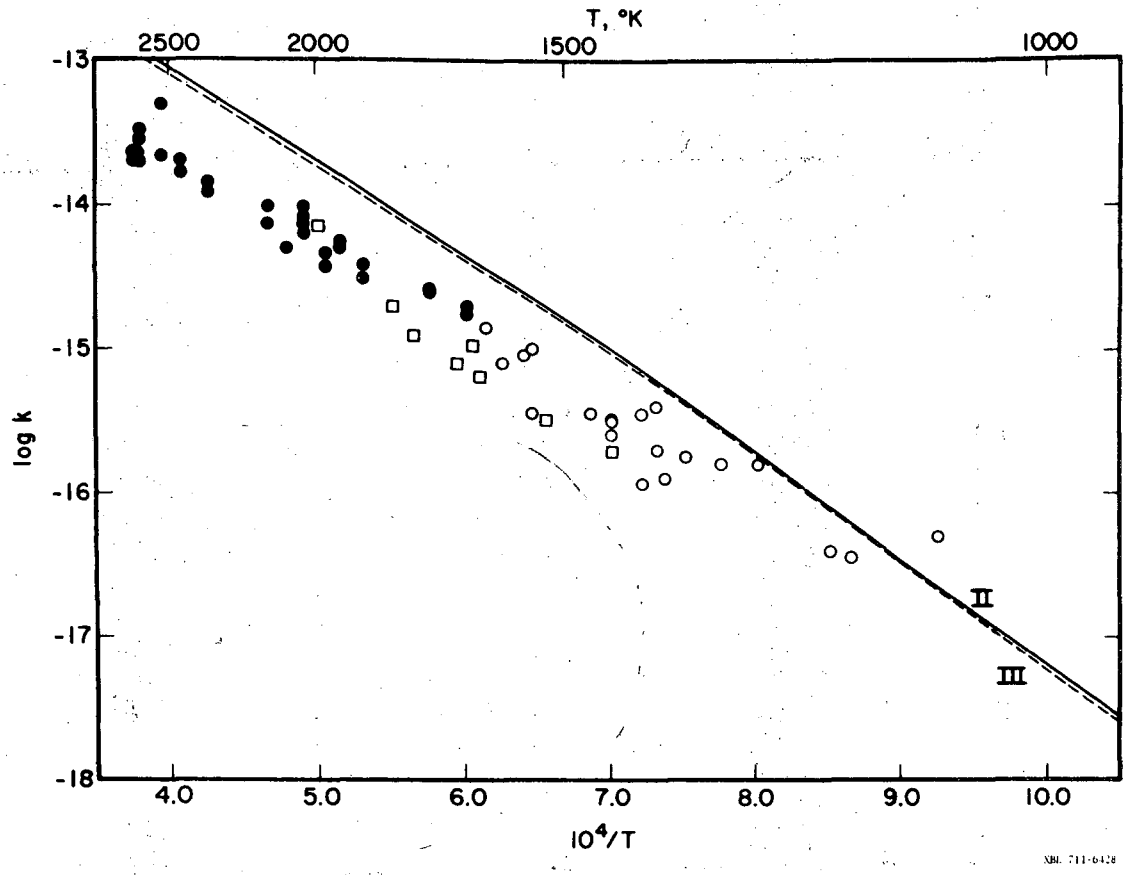
T, °K
2500
2000
1500
1000
-13
-14
-15
-16
-17
-18
log k
4.0
5.0
6.0
7.0
8.0
9.0
10.0
10⁴/T
II
III

Fig. 5

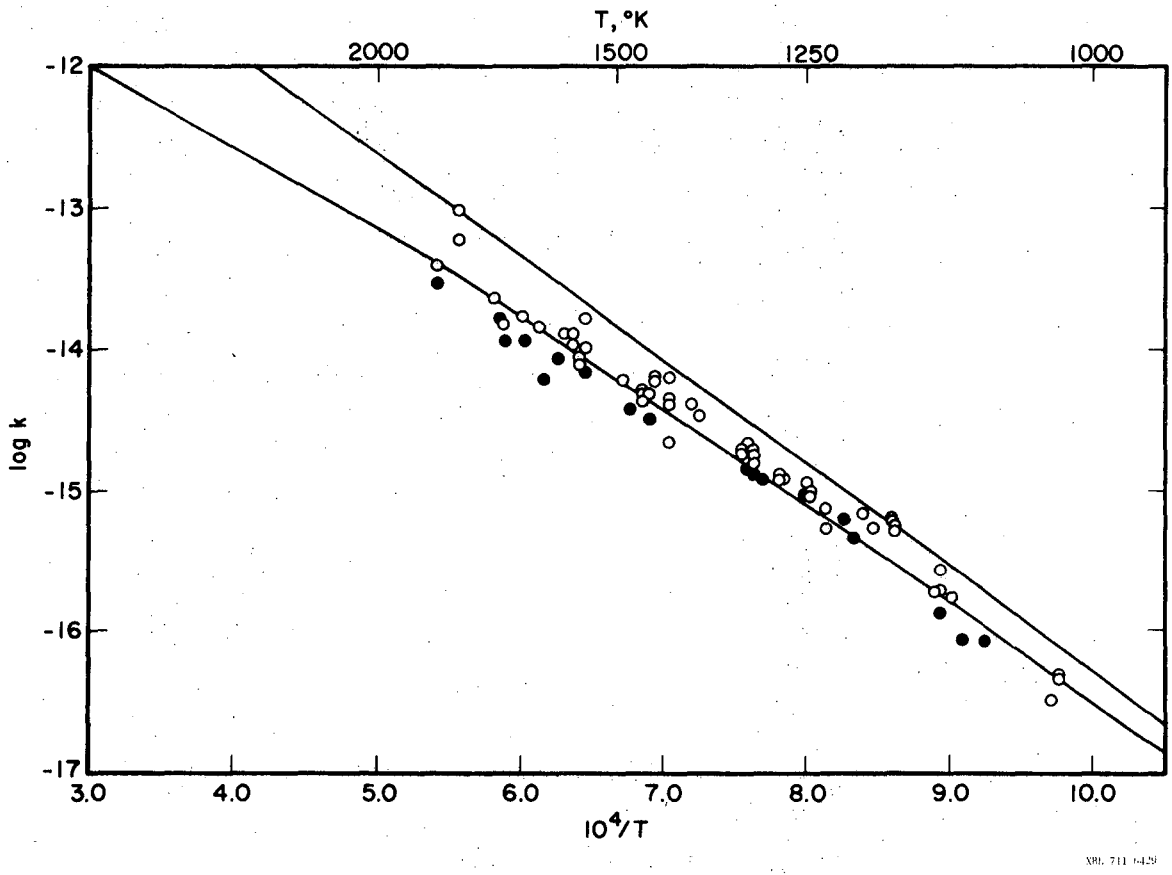
T, °K
2000
1500
1250
1000
-12
-13
-14
-15
-16
-17
log k
3.0
4.0
5.0
6.0
7.0
8.0
9.0
10.0
10⁴/T

Fig. 6A

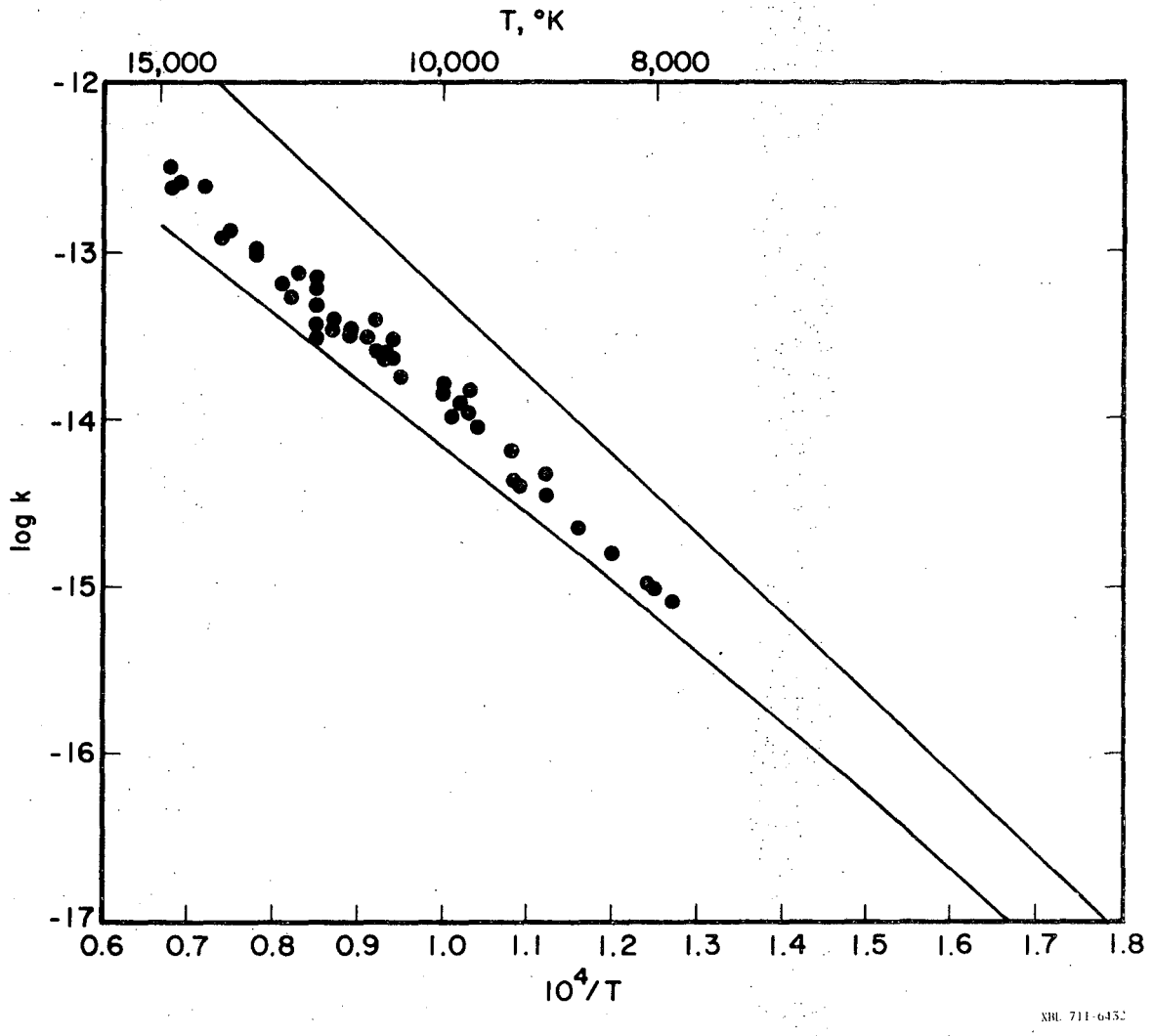
T, °K
15,000
10,000
8,000
-12
-13
-14
-15
-16
-17
log k
0.6
0.7
0.8
0.9
1.0
1.1
1.2
1.3
1.4
1.5
1.6
1.7
1.8
10⁴/T

Fig. 6B

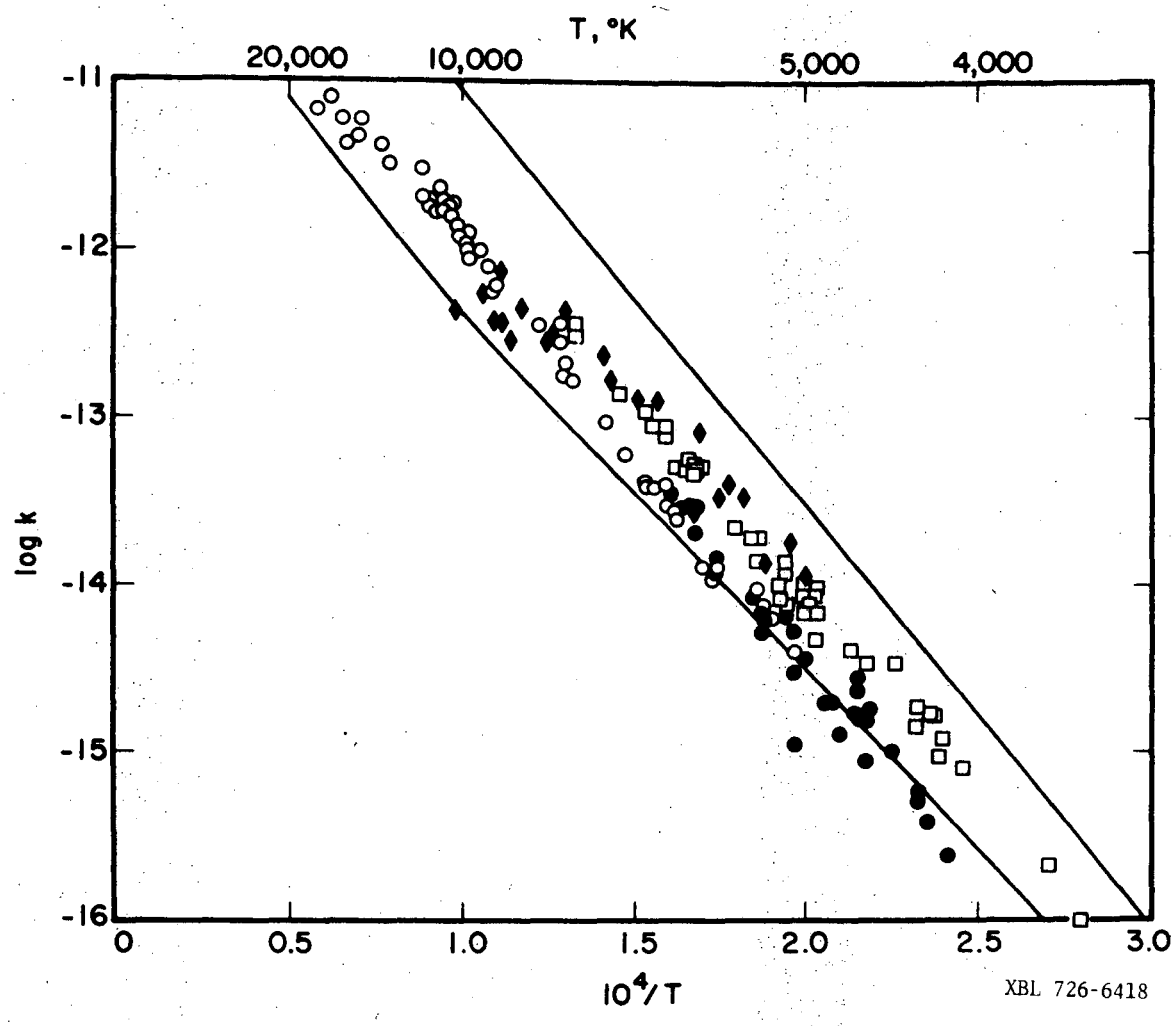
T, °K
20,000
10,000
5,000
4,000
-11
-12
-13
-14
-15
-16
log k
0
0.5
1.0
1.5
2.0
2.5
3.0
10⁴/T
XBL 726-6418

Fig. 6C

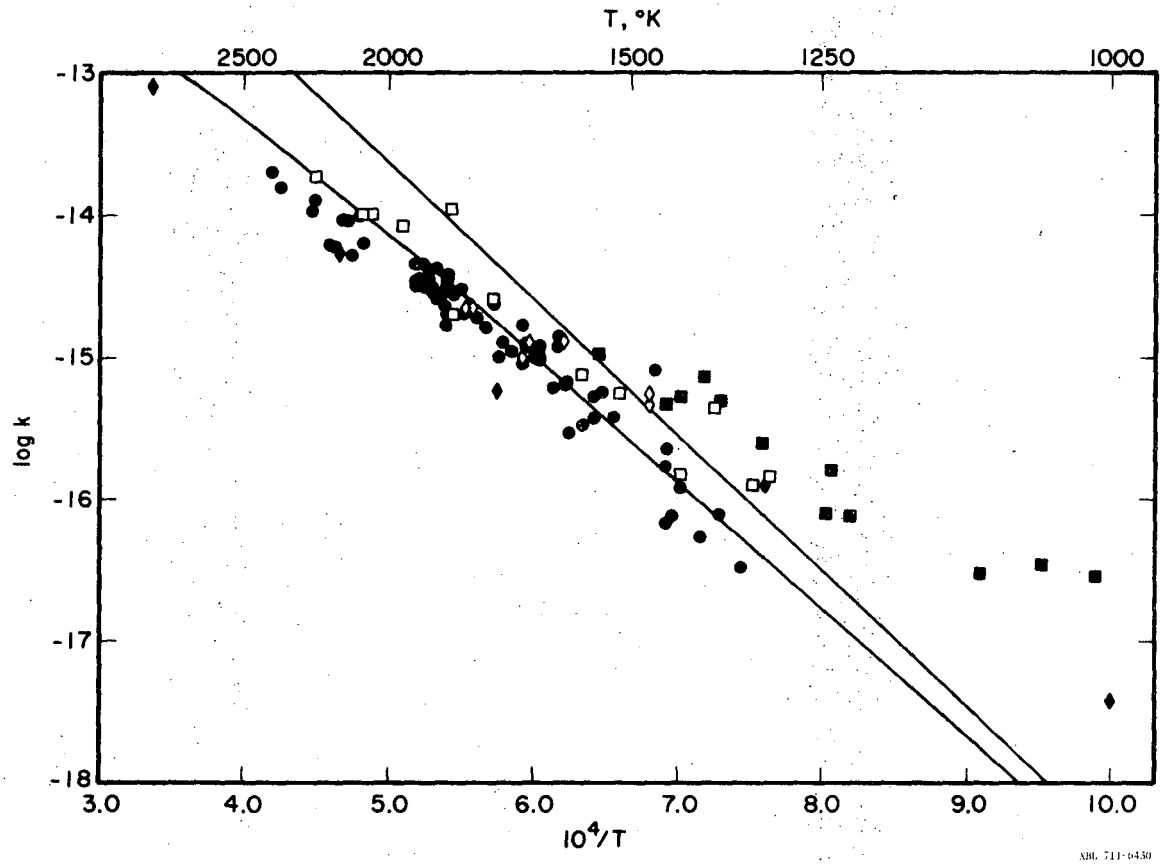
T, °K
2500
2000
1500
1250
1000
-13
-14
-15
-16
-17
-18
log k
3.0
4.0
5.0
6.0
7.0
8.0
9.0
10.0
10⁴/T
XBL 711-0430

Fig. A1

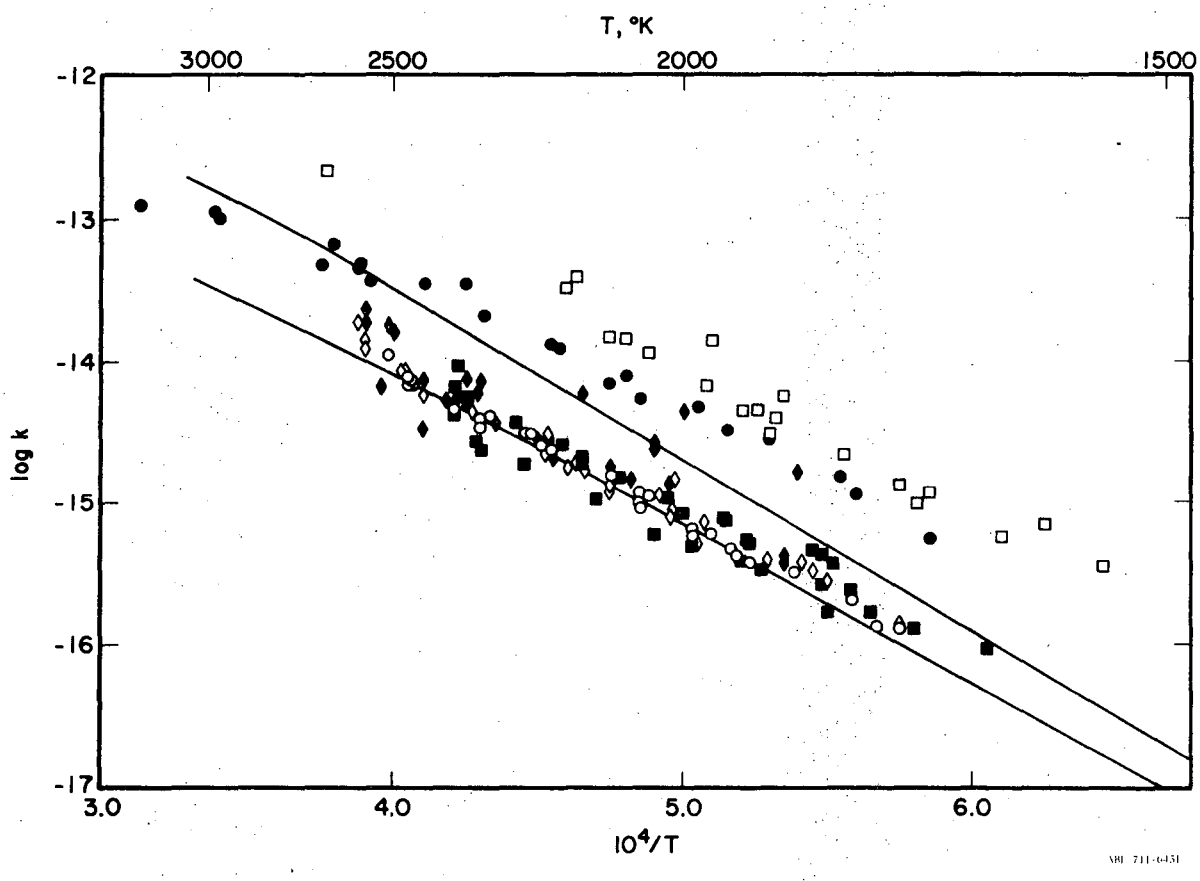

Fig. A2

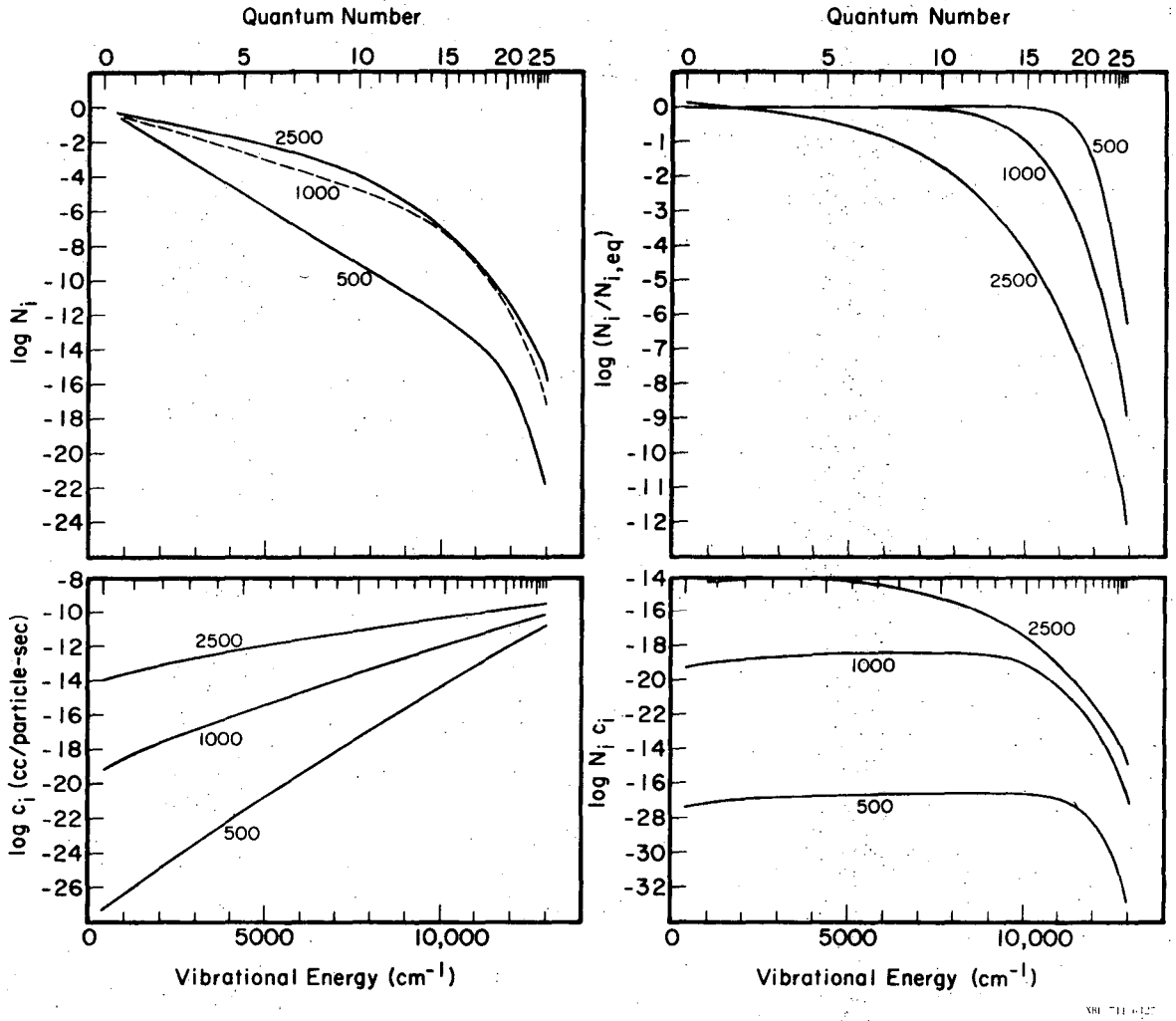
Quantum Number
0 5 10 15 20 25
log N_i
2500
1000
500
log $(N_i/N_{i,eq})$
log c_i (cc/particle-sec)
log N_i c_i
0 5000 10,000
Vibrational Energy (cm^{-1})

Fig. A3

TECHNICAL INFORMATION DIVISION
LAWRENCE BERKELEY LABORATORY
UNIVERSITY OF CALIFORNIA
BERKELEY, CALIFORNIA 94720